EFFECTS OF A DILUENT INERT GAS ON ETHYLENE AND PROPANE BUNSEN FLAMES

J. T. ERK,
H. A. SMITH

1956

EFFECTS OF A DILUENT INERT GAS ON ETHYLENE AND PROPANE BUNSEN FLAMES

Lt. J. T. Erk, U. S. Navy

Lt. H. A. Smith, U. S. Navy

May 15, 1956

SUMMARY

An earlier investigation of flame phenomena at the University of Michigan correlated flame speed with a non-dimensional parameter, the Peclet number. This investigation was undertaken to study the effect of inert diluents on flame speed and to determine whether the above correlation is valid when diluents are introduced into the unburned gases.

A Bunsen burner flame was employed in this investigation using propane and ethylene as fuels. In addition to normal air, four volumetric nitrogen-oxygen ratios were used, ranging from 1.0:1 through 5.75:1. Data was recorded at pressures from one atmosphere down to 1/4 atmosphere, using burner nozzles from 1/8 to 3/4 inches in diameter. For a given fuel and nitrogen-oxygen combination, an endeavor was made to hold constant the following quantities: oxygen-fuel ratio, jet velocity, and flame shape.

As a result of this study, it has been concluded that:

1. The previous correlation of flame speed with Peclet Number holds for the range of diluent inert gases investigated.

2. Flame speed varies inversely with the concentration of the diluent gas.

3. Apparent flame speed diverges more rapidly from true flame speed, at reduced pressures, as the nitrogen concentration is reduced.

4. The slope of the true flame speed envelope varies inversely with nitrogen concentration.

5. By application of adiabatic flame temperatures, it is possible to predict flame speeds throughout the range of diluent concentrations and pressures, knowing only the flame speeds at any two diluent concentrations.

This study was conducted at the University of Michigan, Ann Arbor, Michigan

during the Spring of 1956, under the supervision of Professor R. B. Morrison of the Aeronautical Engineering Department.

SYMBOLS

A	Area, ft^2.
A_e	Activation energy, BTU/mol ^oR.
C	Nitrogen - oxygen ratio, by volume.
C_p	Specific heat, BTU/lb ^oF.
D	Diameter of burner, ft.
K	Thermal conductivity, BTU/sec. ft. ^oF.
P	Pressure, lbs/ft^2 or centimeters of mercury.
P_e	Peclet number, dimensionless.
Q	Volumetric flow rate, ft^3/min.
R	Universal gas constant.
T_f	Adiabatic flame temperature.
T_{f_o}	Adiabatic flame temperature, pure oxygen.
U	Gas stream velocity, ft/sec.
V_{fa}	Apparent normal flame speed, ft/sec.
V_f	True normal flame speed, ft/sec.
V'_{fa}	Apparent flame speed, ft/sec., as computed from the adiabatic flame temperature approach, eq. (5).
ρ	Density at standard temperature and pressure, lbs/ft^3.

Subscripts

B	At burner.
std	Standard temperature and pressure, 14.7 psi, 520^{o}R.

INTRODUCTION

A previous study conducted at the University of Michigan[1] demonstrated that the flame propagation rate in propane - air and ethylene - air Bunsen flames could be correlated with a non-dimensional parameter, the Peclet number. The writer reviewed some of the basic theory of the flame propagation phenomenon and explained the mechanism by which burner size and reduced pressure change the apparent flame speed from the true flame speed which would be observed for a very large burner at a given pressure. He demonstrated that the apparent flame speed for different sized burners converges, at high Peclet numbers, on an envelope of true flame speed over the range of pressures investigated. This envelope of true flame speed appears as a straight line when plotted on a graph of flame speed versus the logarithm of the pressure. The relationship between Peclet number and flame speed was expressed mathematically as: $V_{fa} / V_f = 1 - e^{-Pe\beta}$ where β is a constant depending upon the reactants. It was concluded that: (1) the normal flame speed for the fuels studied varied inversely with the logarithm of the pressure from atmospheric pressures to as low as one inch Hg. absolute, and (2) the Peclet number must be kept large to avoid considerable reductions in flame speeds at sub-atmospheric pressure.

The purpose of the present investigation is: (1) to determine whether the foregoing conclusions remain valid when the diluent nitrogen concentration in the combustible mixture is varied, and (2) to make a quantitative survey of how the flame propagation rate in the previously mentioned hydrocarbons is affected by the diluent nitrogen. For this purpose five nitrogen - oxygen mixtures were burned with each of the fuels, the minimum diluent nitrogen being 50% and the

maximum 85% by volume in the "air" reacting with the fuel.

The work was conducted at the University of Michigan in the Aeronautical Engineering propulsion laboratory, East Engineering Building, during January, February and March 1956. It was performed as part of the third year curriculum in Aeronautical Engineering of the U. S. Naval Postgraduate School, Monterey, California, as partial fulfillment of the requirements for a Master of Science degree. It was financed by the Bureau of Aeronautics, Navy Department, Washington, D. C.

We would like to express our appreciation to Professor R. B. Morrison for his overall guidance and enthusiastic interest in the project. Professor T. C. Adamson, Mr. R. E. Cullen, and Mr. M. L. Gluckstein also contributed many helpful suggestions which are greatly appreciated. To the Department of Chemistry and Metallurgy at the University of Michigan go our thanks for their generous assistance in the field of mass spectroscopy.

EQUIPMENT AND PROCEDURE

The apparatus herein described was provided by the University of Michigan, having been employed in previous combustion studies. A line diagram, presented in Fig. 1, illustrates the configuration as employed in this investigation.

The burner assembly consisted of a stainless steel tube approximately two inches in diameter, 24 inches long, and one-quarter inch thick. The combustible mixtures were introduced at the bottom of the tube through a three-quarter inch flexible line. The top of the tube was internally threaded to provide for interchangeable burner nozzles with nominal inside diameters from one-eighth inch to 1 1/4 inches. Screens just below the burner nozzles insured a constant low-level of turbulence in the flow and assisted in preventing flash-backs into the fuel lines. The upper four-inch portion of the burner tube was water-jacketed to provide the burner with as near a constant temperature as possible. Ignition of the mixture was accomplished by a high voltage, movable electrode at the burner nozzle.

The pressure chamber, within which the burner assembly was mounted, was one foot in diameter and three feet high. A 100-centimeter mercury manometer measured the pressure within the chamber. Sub-atmospheric pressures were maintained at desired levels with a Nash-Hytor vacuum pump. Manual control over the pressure level was exercised through a series of bleed lines and control valves in the vacuum lines. Two 1" x 7" diameter plate glass windows permitted visual inspection and photographing of the flame.

A box camera was mounted on the pressure chamber at one of the windows. After obtaining optimun conditions of focus and parallax, the camera was locked into position to restrain further motion. Royal Pan 4" x 5" sheet film

was employed, with exposures ranging from f4 to f6.3 at 1/25 to 1/50 of a second.

Because of the explosive nature of premixed combustibles, the fuel and nitrogen-oxygen supplies were stored in separate tanks. The flows were metered through individual rotameters, calibrated at standard conditions, and were united immediately downstream. Complete mixing was obtained by flow of the gases through several inches of tightly packed steel wool, this device also acting as a flame trap in case of flash-back.

For any given fuel and oxygen-nitrogen mixture, data was recorded at pressures of 1, 3/4, 1/2, and 1/4 atmospheres. For each run, fuel-oxygen ratio and nozzle velocity were held constant while attempting to maintain similar geometric flame shapes. The fuel-oxygen ratio was that which gave maximum flame speed and was determined experimentally at atmospheric pressure prior to the run for each mixture. Although the fuel-air ratio for maximum flame speed varies slightly with pressure, this effect is secondary, according to Ref. 2. The nozzle velocity was that which provided a nearly constant geometric flame shape throughout the range of pressures and burner sizes. At each pressure level, the flame was photographed and the following data recorded: rotameter flow rates, pressures and temperatures; chamber pressure; and room temperature and pressure. According to Ref. 1, the temperature of the unburned gases at the burner lip varies approximately 10 degrees, with negligible effect upon the results. In the calculations, this value was taken as constant at 85° F.

The photographs were enlarged by factors of 10 to 40, depending upon original flame size. The average normal flame speed was computed from the

equation

$$V_{fa} = \frac{Q_B}{A_f} \tag{1}$$

where Q_B is the volumetric flow rate of the unburned gases at the burner lip and A_f is the area of the inner reaction zone of the flame. This area was computed from the Theorem of Pappas:

$$A_f = 2\pi L\bar{x} \tag{2}$$

where L is the length of the inner reaction zone from base to tip of the photographed flame, and $\bar{x}$ is the centroid of L with respect to the longitudinal axis of the flame.

This investigation was limited to two fuels, ethylene and propane, the former being an unsaturated double-bond hydrocarbon and the latter a saturated single-bond hydrocarbon. The volumetric ratios of nitrogen to oxygen used with each fuel were 1.0 : 1, 1.8 : 1, 3.76 : 1, 4.74 : 1, and 5.75 : 1. These mixtures were prepared by the method of partial pressures and verified with mass-spectroscopic analyses. The ethylene, propane, nitrogen and oxygen used in this study had a guaranteed purity of 99% or greater.

A serious limitation in the execution of this study was the inability of the rotameters to measure accurately very low rates of flow. In order to maintain constant burner velocity, flow rates decrease with decreasing pressure. With the smaller burners, the desired flow rate was too low for the smallest rotameter available, and it was therefore impossible to obtain data at the lower pressures with these burners. Attempts to rectify this condition by employing larger burners failed in many cases because of rotameter limitations in the high ranges at the higher pressures or because of the onset of turbulence in the flames.

This limitation might have been prevented had facilities been available for the use of premixed fuels, thus eliminating the necessity of two separate rotameter systems, both required to meter a wide range of flows.

RESULTS AND DISCUSSION

Due to the limitation described under EQUIPMENT AND PROCEDURE, the results in many regions were inadequate for presentation in their original form. In addition, considerable effort was expended in obtaining data at the lowest pressures. Although these points are of interest, they are not as critical in the results as are those at high Peclet numbers, i.e., high pressures. A multitude of points in these latter regions could have been obtained, with less emphasis on those at low pressures, had this effect been realized at an early date. As a consequence, it was impossible to arrive at a simple plot of flame speed versus pressure, and obtain the envelope of true flame speed, as shown in Figs. 5 and 6 of Ref. 1. Since this envelope is of paramount interest in obtaining the relationship of flame speed to Peclet number, it was necessary to derive this envelope by two rather indirect processes. These procedures will be outlined in detail later in this discussion.

The Peclet number is the dimensionless parameter which is defined below and is equal to the product of the Reynold's number and the Prandtl number:

$$P_e = \frac{\rho_B V_{fa} D_B}{\mu} \times \frac{C_p \mu}{K}$$

Since C_p/K is relatively constant, it is felt that if the Reynold's number were used instead of the Peclet Number, similar results would be obtained.

A series of photographs have been presented in Figs. 2, 3, 4 and 5 to illustrate the effects of pressure, burner size, nitrogen concentration, and fuel upon Bunsen-type flames. The effect of pressure is shown in Fig. 2. In this series of photographs, which were enlarged equally, the fuel is ethylene, using the 1.8:1 nitrogen-oxygen mixture. Burner jet velocity and fuel-air ratio

were held constant. As pressure decreases, the flame becomes more diffuse, the primary reaction zone increases in thickness, and the luminous secondary reaction zone disappears (not shown). In addition, the flame begins a gradual departure from the burner base, culminated by blow-off at some reduced pressure. Flame size gradually increases, indicating the retardation of flame speed, as calculated by eq. (1).

The effect of burner size is shown in Fig. 3. The fuel, nitrogen concentration, jet velocity, and fuel-air ratio are constant, identical with those of the previous figure. The comparison is between the 1/8" and 3/16" burners at pressures from 1/2 to one atmosphere. The primary effect here is the ability of the larger burner to maintain a nearly constant geometric shape and size as pressure decreases. The attendant characteristic of a greater tenacity for the burner base may also be noted. These effects are attributed to the reduced effect of heat sink in the larger burner. The fact that the overall heat sink effect is reduced can be shown by considering that the heat sink is proportional to the diameter of the burner while the flame area is proportional to the diameter squared.

In Fig. 4 is shown the effect of nitrogen concentration. Since burner size, jet velocity, and fuel-air ratio were variant it is only possible to surmise the effect of nitrogen from the photographs. However, burner size has a negligible effect here since no great changes have occurred in flame shapes between the 3/4 and 1/2 atmosphere points. Likewise, although fuel-air ratios have changed, the fuel-oxygen ratios are within five percent. The greatest change occurred in jet velocity, decreasing from 13 to 2 feet per second as the nitrogen concentrations increased from 64 to 83 percent. This indicates a large decrease in

flame speed, with decrease in reaction rate and flame temperature. The flame became more diffuse, with a reduced secondary reaction zone, and reduced tenacity. These effects are caused by the excess heat lost in raising the temperature of the added diluent from 85°F. to flame temperature.

The effect of fuel is shown in Fig. 5. Here again jet velocity and fuel-air ratio are not identical for the two fuels. The fact that the ethylene reaction rate has increased over that of propane is indicated in the smaller flame sizes, with resulting increases in flame speed. This effect is attributed in part to the lower activation energy of the ethylene fuel. It is also noted that the ethylene flame has greater tenacity and a greater secondary reaction zone (not shown).

In correlating the results of this study with that of Ref. 1, it was desirable to obtain a relationship between flame speed and Peclet number; hence, a plot of apparent flame speed versus Peclet number was made for each of the fuels, using Cullen's data to establish basic trends, i.e., curves of constant burner size and curves of constant pressure. These curves are shown in Figs. 6 and 7. The pressure curves are seen to reach a constant flame speed as Peclet number increases. This ultimate value of apparent flame speed is the true flame speed for that particular pressure and is the value needed to establish the true flame speed envelope on the flame speed versus pressure plots.

From the trends thus established it was possible to draw curves through the few points in each of the N_2/O_2 runs and to make a fair estimation of the true flame speed for each point (Figs. 8 to 13). It is interesting to note that as the amount of diluent is decreased, both the curves of pressure and burner size steepen considerably and appear to peak at higher Peclet numbers. This results in a steeper slope for the true flame speed envelope as nitrogen content decreases.

The plots of apparent flame speed versus pressure, with the estimated true flame speed envelopes, are shown in Figs. 14 - 17.

To take these results a step further, Fig. 18 is a plot of the ratio of V_{f_a}/V_f versus Pe. Although Ref. 1 combined the two fuels on the same graph, it is evident from these graphs of the several concentrations that different curves are obtained for propane and ethylene at each diluent concentration. Increasing diluent concentration results in a translation of the curve to the left.

A second approach to this same problem, which gave similar results, involved consideration of adiabatic flame temperatures and activation energies. Due to the complexity of this approach, only the details involving propane as a fuel will be discussed.

By the method outlined in Ref. 3, the adiabatic flame temperatures were computed for propane at each of the five nitrogen-oxygen concentrations. These temperatures were plotted versus nitrogen-oxygen ratio, as shown in Fig. 19. If it is assumed that this relationship is linear, then the equation relating the variables is

$$T_f = T_{f_o} - kC \qquad (3)$$

where T_{f_o} is the flame temperature with pure oxygen, k is the slope of the curve, and C is the nitrogen-oxygen ratio.

In Ref. 4, it was shown that

$$V_{f_a} \sim e^{-\frac{A_e}{2RT_f}} \qquad (4)$$

where A_e is the activation energy, R is the universal gas constant and V_{f_a} is the apparent flame speed. In this case, a single rate controlling reaction is assumed.

Substituting the relationship of eq. (3) into eq. (4) and letting $a = A_e/2R$,

$$V_{f_a} \sim e^{-\frac{a}{T_{f_o} - kC}}$$

Then

$$\frac{V_{f_a}}{V'_{f_a}} = e^{-a\left(\frac{1}{T_{f_o} - kC} - \frac{1}{T_{f_o} - kC'}\right)} \qquad (5)$$

where V'_{f_a} is the apparent flame speed at any other nitrogen-oxygen ratio, C'.

Then,

$$\ln\left(\frac{V_{f_a}}{V'_{f_a}}\right) = -a\left(\frac{1}{T_{f_o} - kC} - \frac{1}{T_{f_o} - kC'}\right)$$

$$a = \frac{(T_{f_o} - kC)(T_{f_o} - kC')}{k(C' - C)} \ln\left(\frac{V_{f_a}}{V'_{f_a}}\right) \qquad (6)$$

By selecting values at a given Peclet number and burner diameter from the data of this investigation for V_{fa}, V_{fa}', C, and C', a value of "a" may be computed, which by definition, is constant for a given fuel, regardless of the value of C. Then by eq. (5), the apparent flame speeds for any nitrogen-oxygen ratio may be related to those for air, simply by application of appropriate values of C.

Applying this procedure to the four non-air propane flames and plotting the results against logarithmic pressure produced the curves of Fig. 20. The curve for normal air is also included. Next, the envelope for true flame speed of the propane-air mixtures was taken from Fig. 5 of Ref. 1 and plotted. Using this curve in combination with those from each nitrogen-oxygen ratio, it was possible to construct the curves of Fig. 21.

Comparison of the curves of Fig. 18 with those of Fig. 21 reveals a marked similarity. Since the means by which they were constructed were totally unrelated, it is felt that the trends indicated therein are representative of the results to be expected from nitrogen dilution. The effect, as stated earlier is as follows; for increased nitrogen, the apparent flame speed approaches the true flame speed at Peclet numbers lower than those for air, while for decreased nitrogen, the apparent flame speed approaches the true flame speed at Peclet numbers higher than those for air.

Although it has become apparent that there exists a separate curve for each nitrogen concentration and each fuel, this fact does not invalidate the previous correlation of Peclet number with flame speed, as proposed in Ref. 1. Each of the curves of Figs. 18 and 21 is still a close approximation to the general expression:

$$V_{fa}/V_f = 1-e^{-P_e \beta}$$

as developed in Ref. 1. The variation is due to the "constant", β, which takes on new values for each fuel and each nitrogen concentration. Knowing the flame speed of a given fuel with air and with a second nitrogen-oxygen mixture, it is possible to obtain the value of β for this fuel and any other nitrogen-oxygen mixture, using the adiabatic flame temperature approach (eq. 5).

For a number of reasons, it must be emphasized that these results are, for the most part, qualitative only. There were several sources of error in this investigation and the degree of error is unknown in some instances. As an example, consider the case of computing flame areas, where the most critical area, the base of the flame, is the most difficult to determine due to loss of luminosity in the diffusion zone. Even with care and good judgment,

the determination is difficult, and probably best obtained by averaging the results of a number of separate runs. For the time allotted, this procedure was not acceptable, and it is therefore possible that an error of 20% could exist in some of the results presented herein. Other sources of error existed in the analyses of the nitrogen-oxygen mixtures, the flow rates indicated by the rotameters, particularly at the lower limits, and the assumption that the gas temperature at the burner remained constant at 85°F. Compared with the error incurred in computation of flame areas, these are all very small and therefore insignificant.

A tabulation of the results is presented in Appendix I, and a complete set of calculations for a typical run is presented in Appendix II.

CONCLUSIONS

For the range of pressures and nitrogen-oxygen ratios investigated, it is concluded that:

1. The extensions of the classic Mallard-Le Chatelier model, as proposed in Ref. 1, is applicable to flames with diluent gases in ratios other than those found in air.

2. The apparent flame speed for the fuels investigated varies inversely with the amount of diluent present.

3. The apparent flame speed diverges more rapidly from the true flame speed, at reduced pressures, as the nitrogen concentration is reduced.

4. The slope of the true flame speed envelope varies inversely with nitrogen concentration; i.e., the true flame speed with pure oxygen decreases more rapidly than it would with air as pressure increases.

5. By application of the adiabatic flame temperature approach, it is possible to predict flame speeds throughout the range of diluent concentrations and pressures, knowing only the flame speeds at two different diluent concentrations.

RECOMMENDATIONS

Since the foregoing conclusions were made from observed trends rather than from a number of experimental points, it is felt that further experiments in this subject should be undertaken to provide more conclusive evidence. If this should be done, the following recommendations may be of assistance:

1. Use premixed fuel and nitrogen-oxygen concentrations to remove the necessity of metering separate flows. This will allow a wider range of data.

2. For a given diluent concentration, obtain data at frequent intervals in the regions of high Peclet numbers for each of four or more burner sizes. This will determine the true flame speed envelope more precisely.

3. Continue to record data at pressures of 1/4, 1/2 and 3/4 atmospheres to insure accurate plots in the regions of low Peclet number.

REFERENCES:

1. Cullen, R. E., "A Nondimensional Correlation of Flame Propagation at Subatmospheric Pressures," Trans ASME, Jan. 1953.
2. Lewis, B., and von Elbe, G., "Combustion, Flames, and Explosions," Academic Press, Inc., New York, 1951.
3. Wenner, R. R., "Thermochemical Calculations," Mc Graw-Hill Book Company, New York, N. Y., 1951.
4. von Karman, T., and Penner, S. S., "Fundamental Approach to Laminar Flame Propagation;" "Selected Combustion Problems;" Butterworth's Scientific Publications, London, 1954.

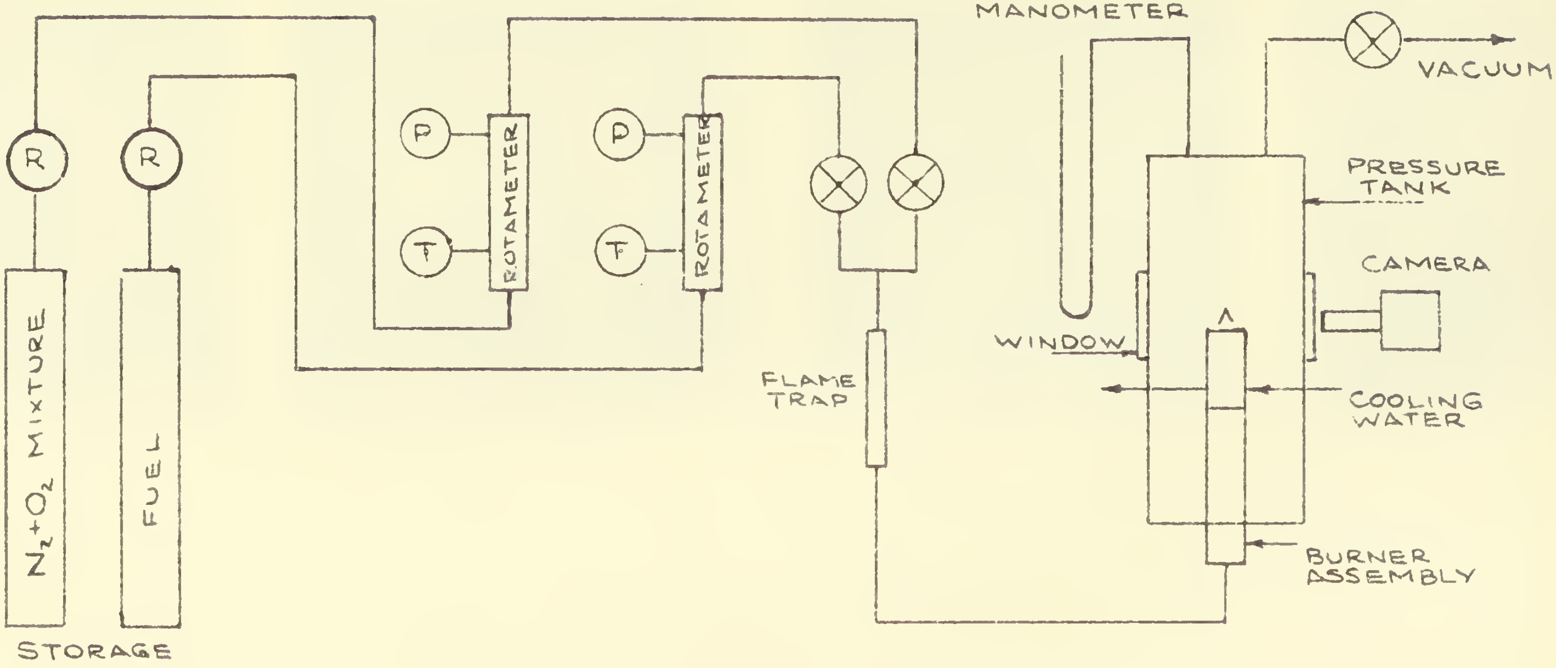

Fig. 1. Block Diagram of Apparatus

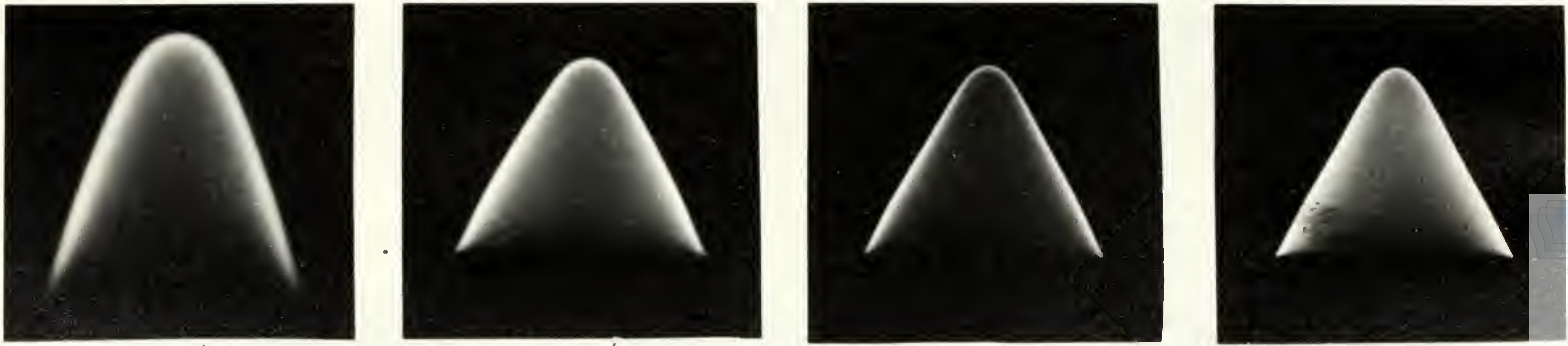

Run #89. 1/4 atm.
V_{f_a} 3.07 fps

Run #88. 1/2 atm.
V_{f_a} 4.36 fps

Run # 87. 3/4 atm.
V_{f_a} 4.89 fps

Run #90. 1 atm.
V_{f_a} 4.84 fps

Fig. 2 Effect of Pressure on Ethylene Bunsen Flames
N_2/O_2 ratio 1.8/1. A/F ratio 7.29/1. D_B 3/16 inch.
U_B 13.1 fps

Run #93. 1/2 atm.
V_{f_a} 3.23 fps
D_B 1/8 in.

Run #92. 3/4 atm.
V_{f_a} 4.04 fps
D_B 1/8 in.

Run #91. 1 atm.
V_{f_a} 4.65 fps
D_B 1/8 in.

Run #88. 1/2 atm.
V_{fa} 4.36 fps.
D_B 3/16 in.

Run #87. 3/4 atm.
V_{fa} 4.89 fps
D_B 3/16 in.

Run #90. 1 atm.
V_{fa} 4.84 fps
D_B 3/16 in.

Fig. 3 Effect of Burner Size on Ethylene Bunsen Flames
N_2/O_2 ratio 1.8/1. A/F ratio 7.29/1. U_B 13.1 fps.

Run #88. 1/2 atm. D_B 3/16 in.
O_2/F ratio 2.61/1. U_B 13.1 fps.
V_{fa} 4.36 fps. N_2/O_2 1.8/1

Run #87. 3/4 atm. D_B 3/16 in.
O_2/F ratio 2.47/1. U_B 13.1 fps.
V_{fa} 4.89 fps. N_2/O_2 1.8/1.

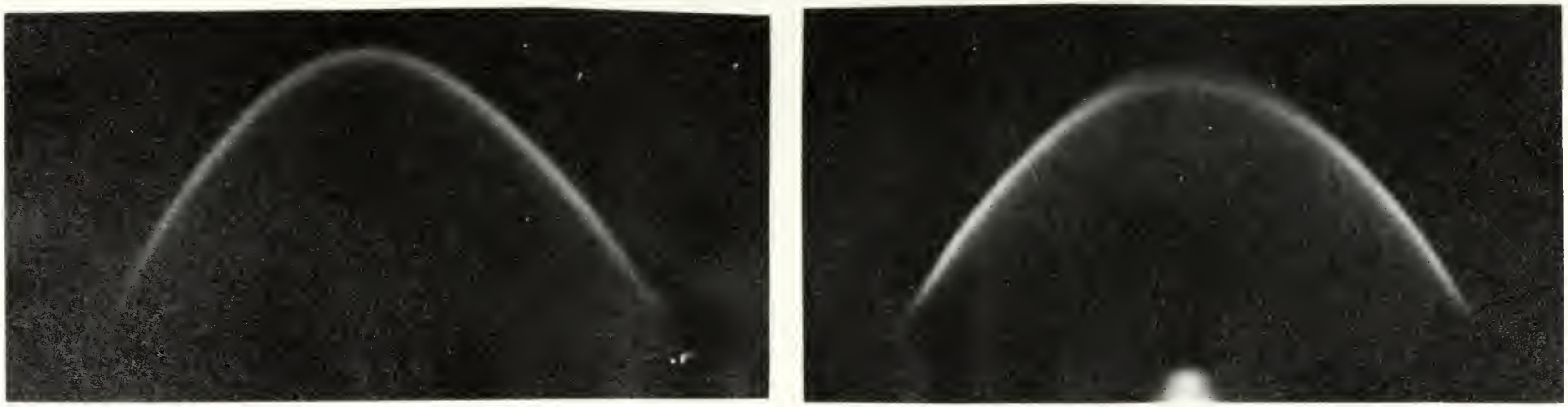

Run #56. 1/2 atm. D_B 3/8 in.
O_2/F ratio 2.45/1. U_B 2.02 fps.
V_{fa} 0.94 fps. N_2/O_2 4.74/1.

Run #54. 3/4 atm. D_B 3/8 in.
O_2/F ratio 2.47/1. U_B 2.02 fps.
V_{fa} 0.96 fps. N_2/O_2 4.74/1.

Fig. 4 Effect of N_2/O_2 Ratio on Ethylene Bunsen Flames

Run #88. Ethylene.
1/2 atm. V_{fa} 4.36 fps.

Run #87. Ethylene.
3/4 atm. V_{fa} 4.89 fps.

Run #90. Ethylene.
1 atm. V_{fa} 4.84 fps.

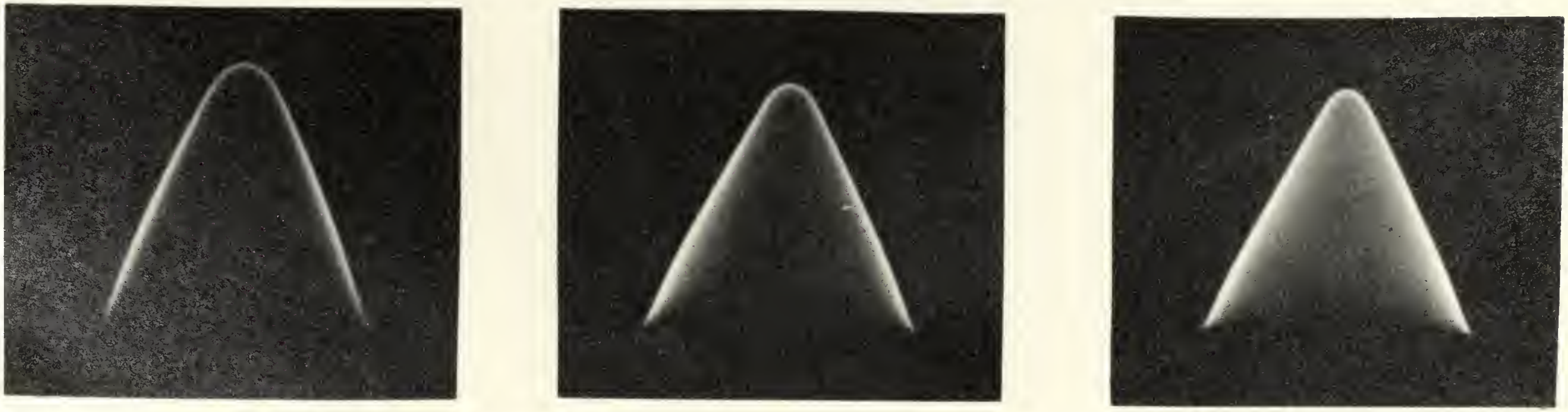

Run #82. Propane.
1/2 atm. V_{fa} 2.50 fps.

Run #81. Propane.
3/4 atm. V_{fa} 2.98 fps.

Run #80. Propane.
1 atm. V_{fa} 3.10 fps.

Fig. 5 Ethylene and Propane Bunsen Flames
D_B 3/16 in. N_2/O_2 ratio 1.8/1.

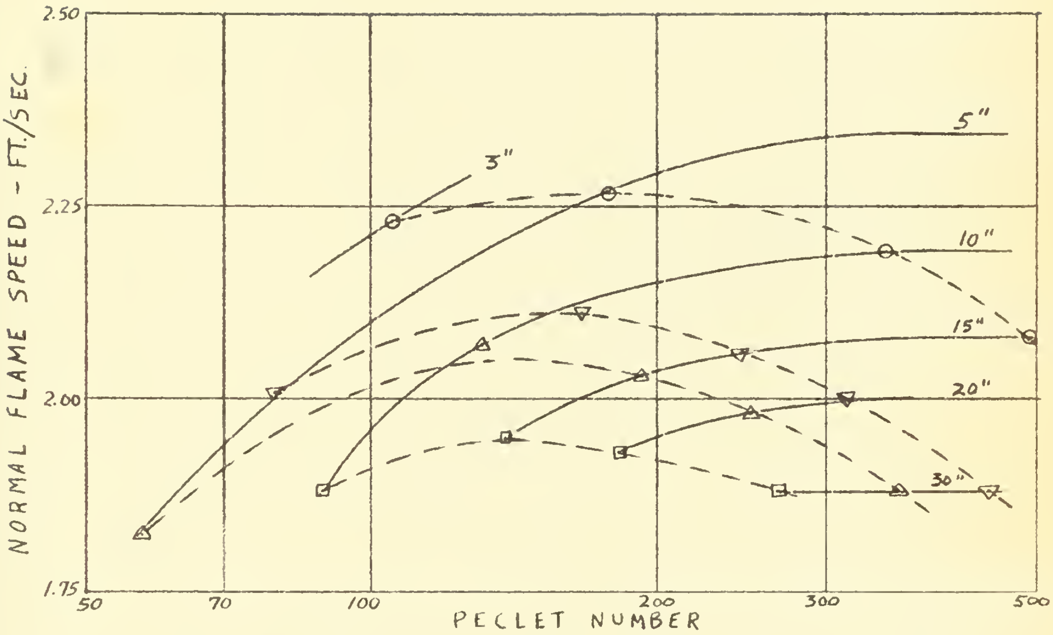

FIG. 6. GRAPH OF FLAME SPEED WITH PECLET NUMBER FOR ETHYLENE - AIR BUNSEN FLAMES. DATA FROM REF. 1 N_2/O_2 3.76/1

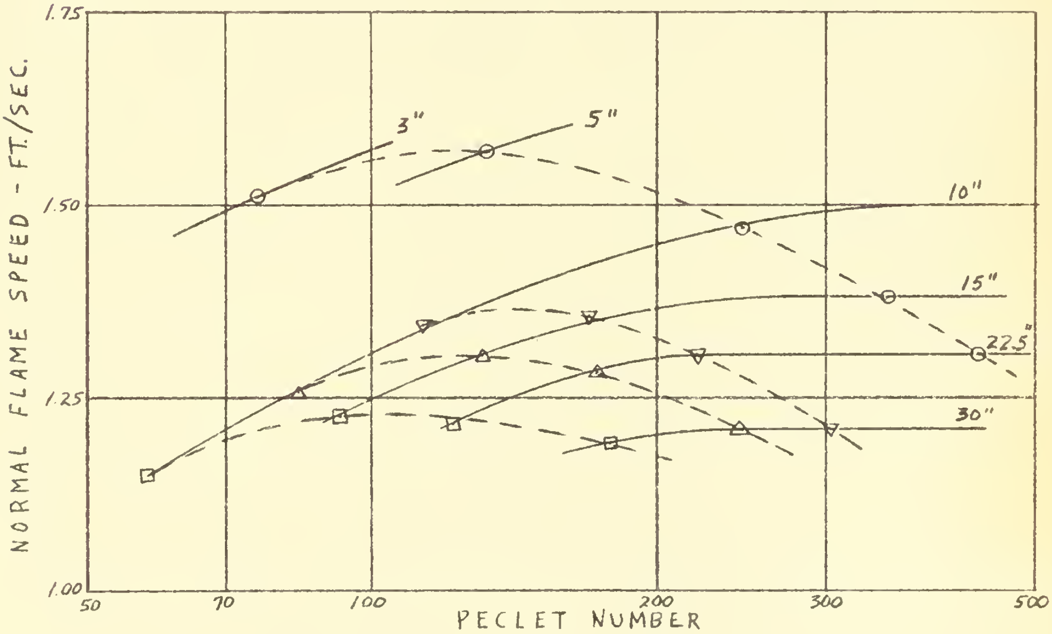

FIG. 7. GRAPH OF FLAME SPEED WITH PECLET NUMBER FOR PROPANE - AIR BUNSEN FLAMES. DATA FROM REF. 1 N_2/O_2 3.76/1

BURNER SIZE ⊡ 3/8", △ 1/2", ▼ 5/8", ⊙ 1 1/4"

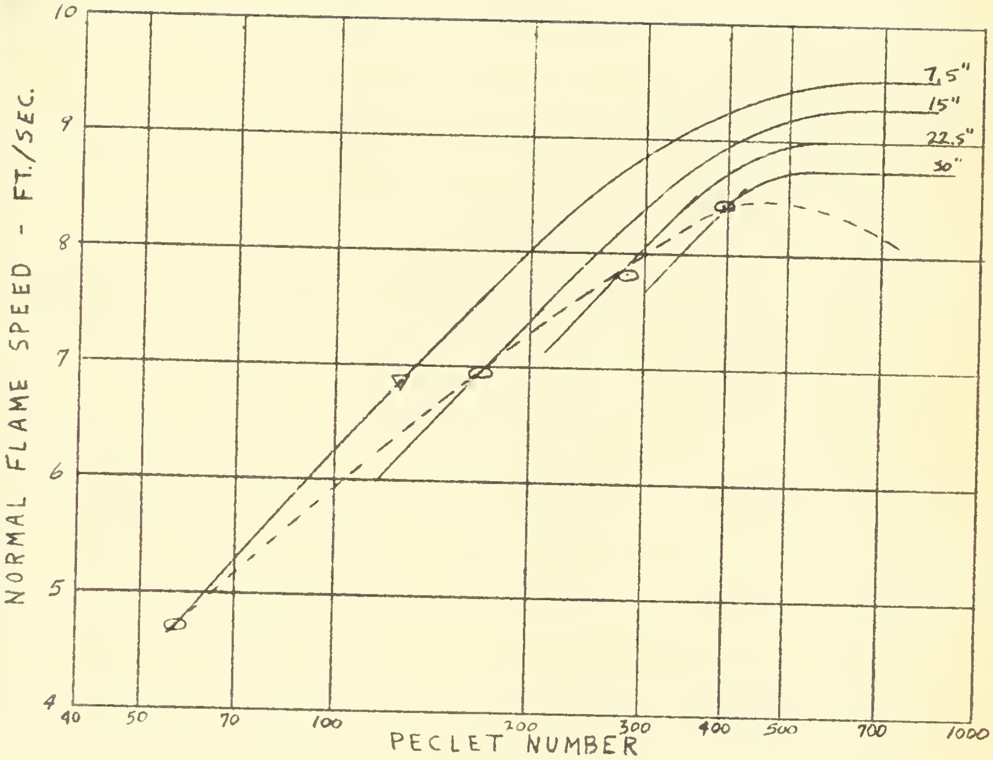

FIG. 8. GRAPH OF FLAME SPEED WITH PECLET NUMBER FOR ETHYLENE - NITROGEN - OXYGEN BUNSEN FLAMES. N_2/O_2 1/1

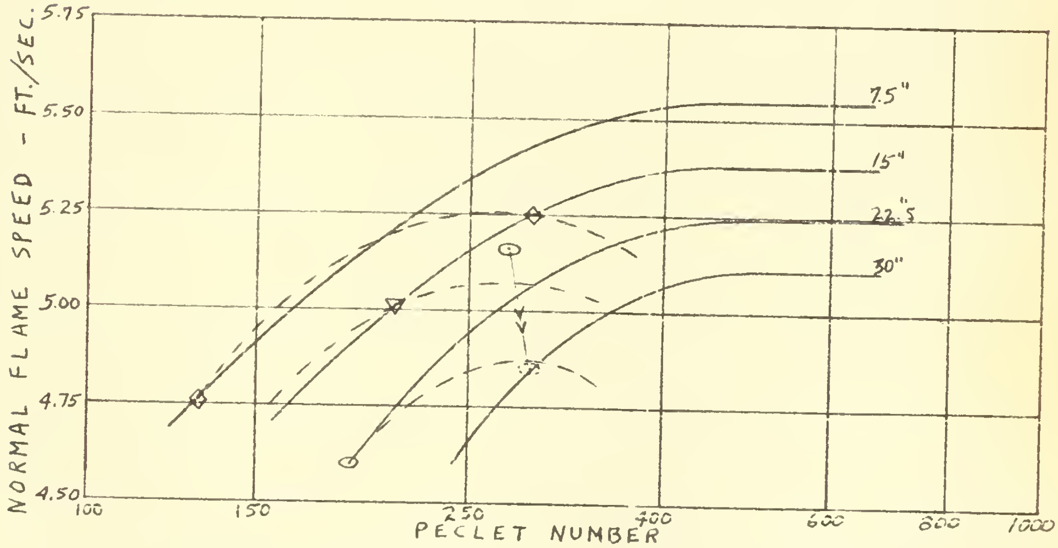

FIG. 9. GRAPH OF FLAME SPEED WITH PECLET NUMBER FOR PROPANE - NITROGEN - OXYGEN BUNSEN FLAMES. N_2/O_2 1/1

BURNER SIZE AS BEFORE

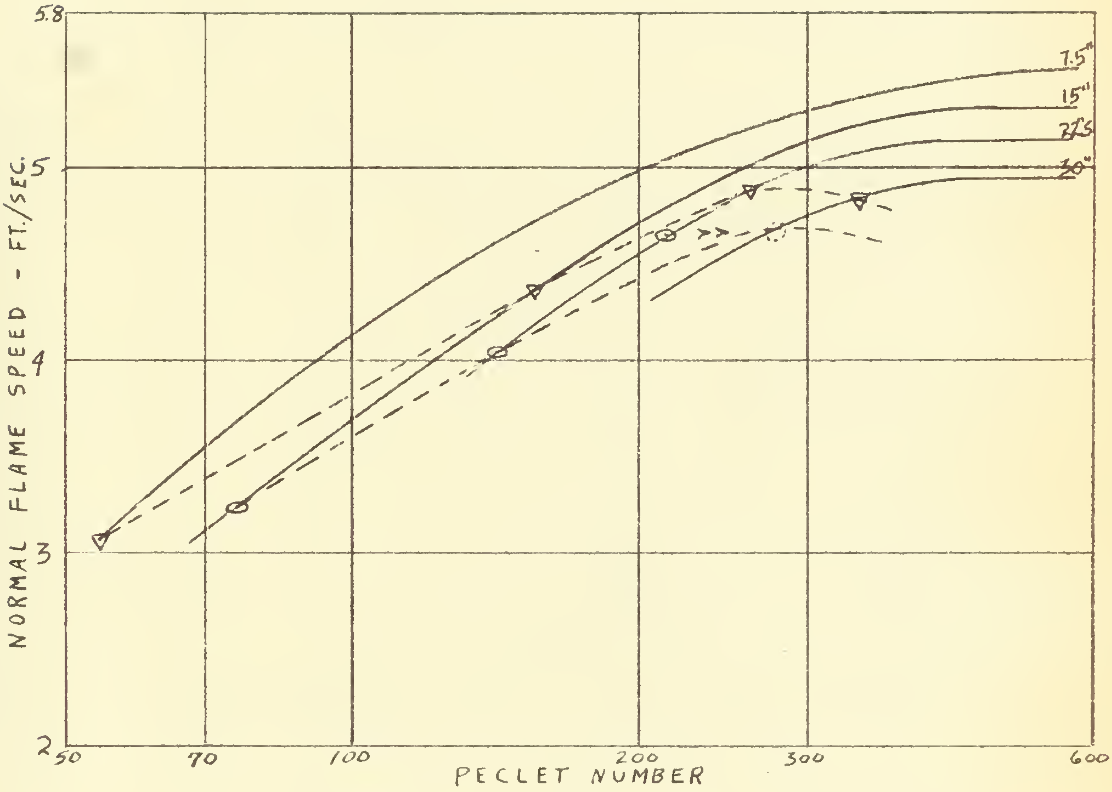

FIG. 10. GRAPH OF FLAME SPEED WITH PECLET NUMBER FOR ETHYLENE - NITROGEN - OXYGEN BUNSEN FLAMES. N_2/O_2 1.8/1

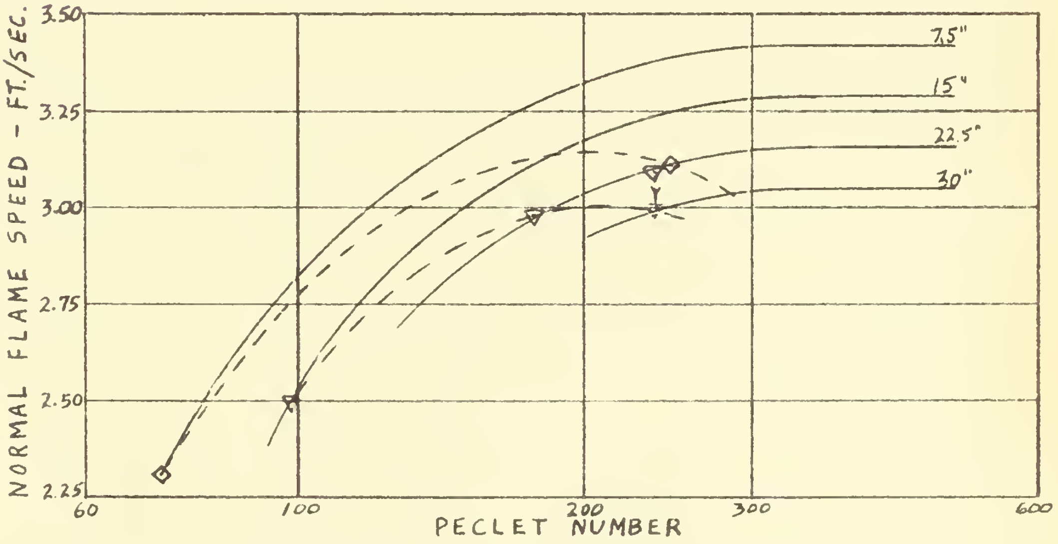

FIG. 11. GRAPH OF FLAME SPEED WITH PECLET NUMBER FOR PROPANE - NITROGEN - OXYGEN BUNSEN FLAMES N_2/O_2 1.8/1

BURNER SIZE AS BEFORE

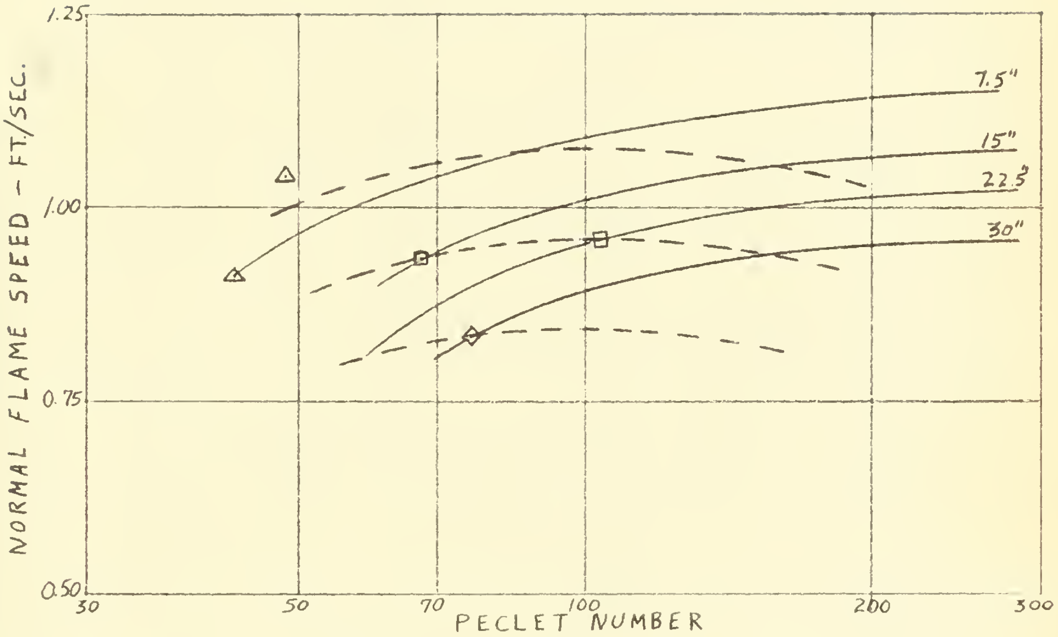

FIG. 12. GRAPH OF FLAME SPEED WITH PECLET NUMBER FOR ETHYLENE - NITROGEN - OXYGEN BUNSEN FLAMES. N_2/O_2 4.74/1

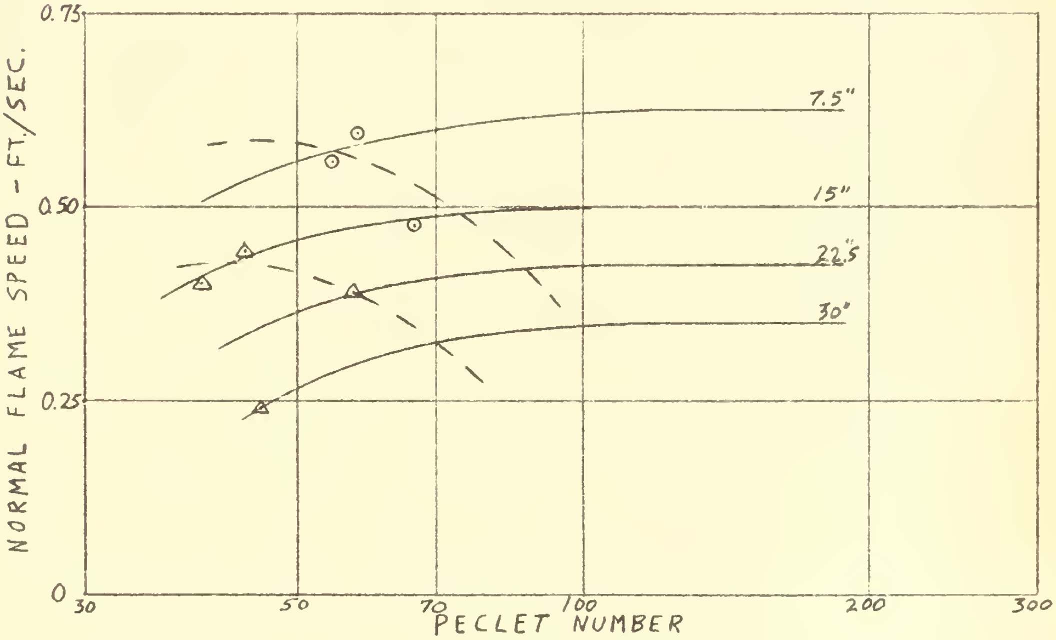

FIG. 13. GRAPH OF FLAME SPEED WITH PECLET NUMBER FOR PROPANE - NITROGEN - OXYGEN BUNSEN FLAMES. N_2/O_2 5.75/1

BURNER SIZE AS BEFORE

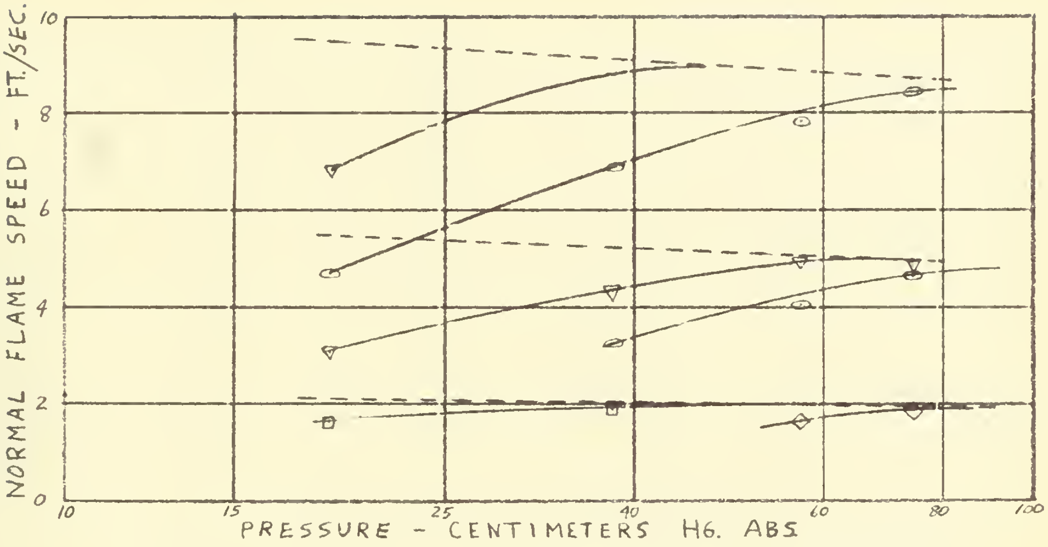

FIG. 14. GRAPH OF FLAME SPEED WITH PRESSURE FOR ETHYLENE - NITROGEN - OXYGEN BUNSEN FLAMES. N_2/O_2 1/1, 1.8/1, 3.76/1

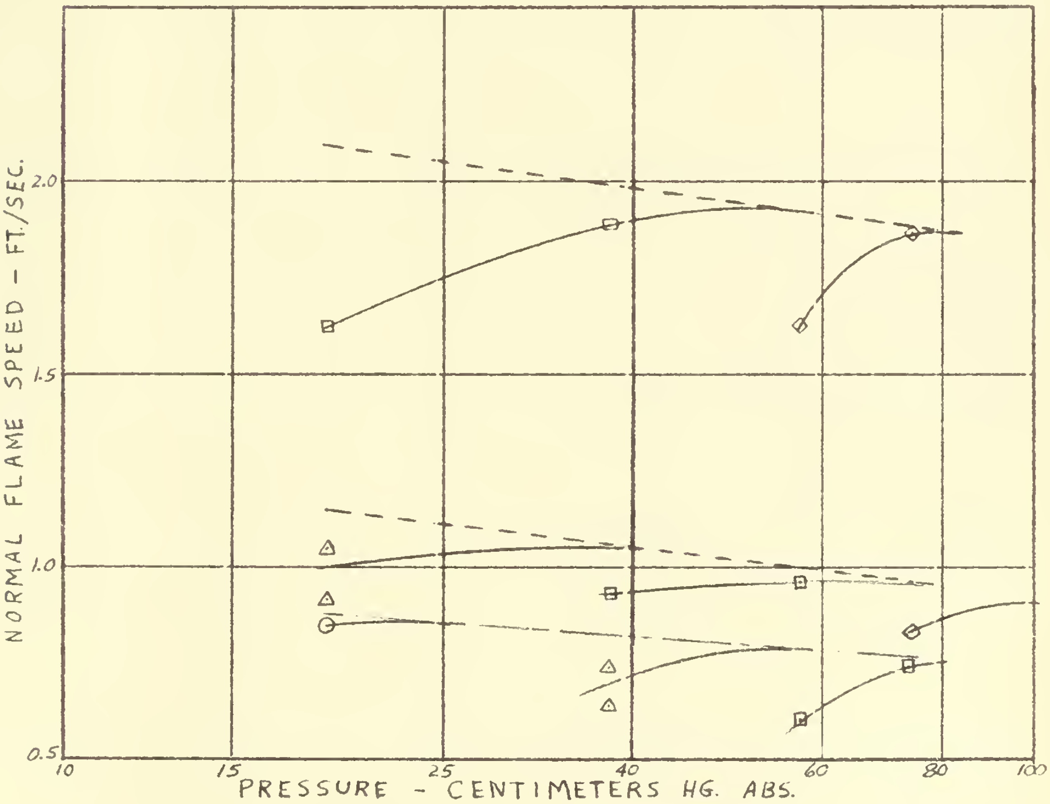

FIG. 15. GRAPH OF FLAME SPEED WITH PRESSURE FOR ETHYLENE - NITROGEN - OXYGEN BUNSEN FLAMES. N_2/O_2 3.76/1, 4.74/1, 5.75/1

BURNER SIZE ⊖ 1/8", ▽ 3/16", ◇ 1/4", ⊡ 3/8", △ 1/2", ⊙ 3/4"

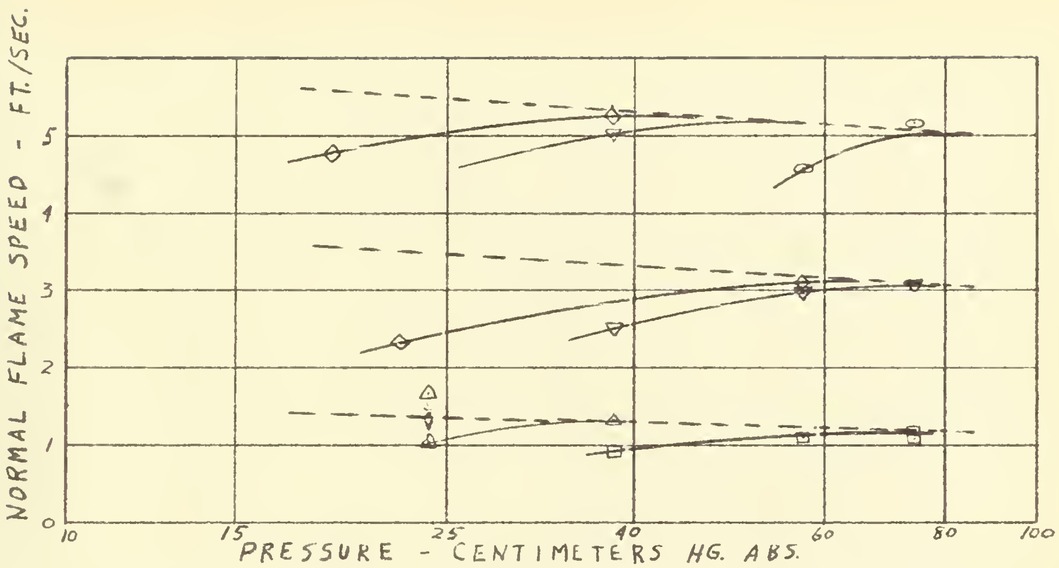

FIG. 16. GRAPH OF FLAME SPEED WITH PRESSURE FOR PROPANE - NITROGEN - OXYGEN BUNSEN FLAMES. N_2/O_2 1/1, 1.8/1, 3.76/1

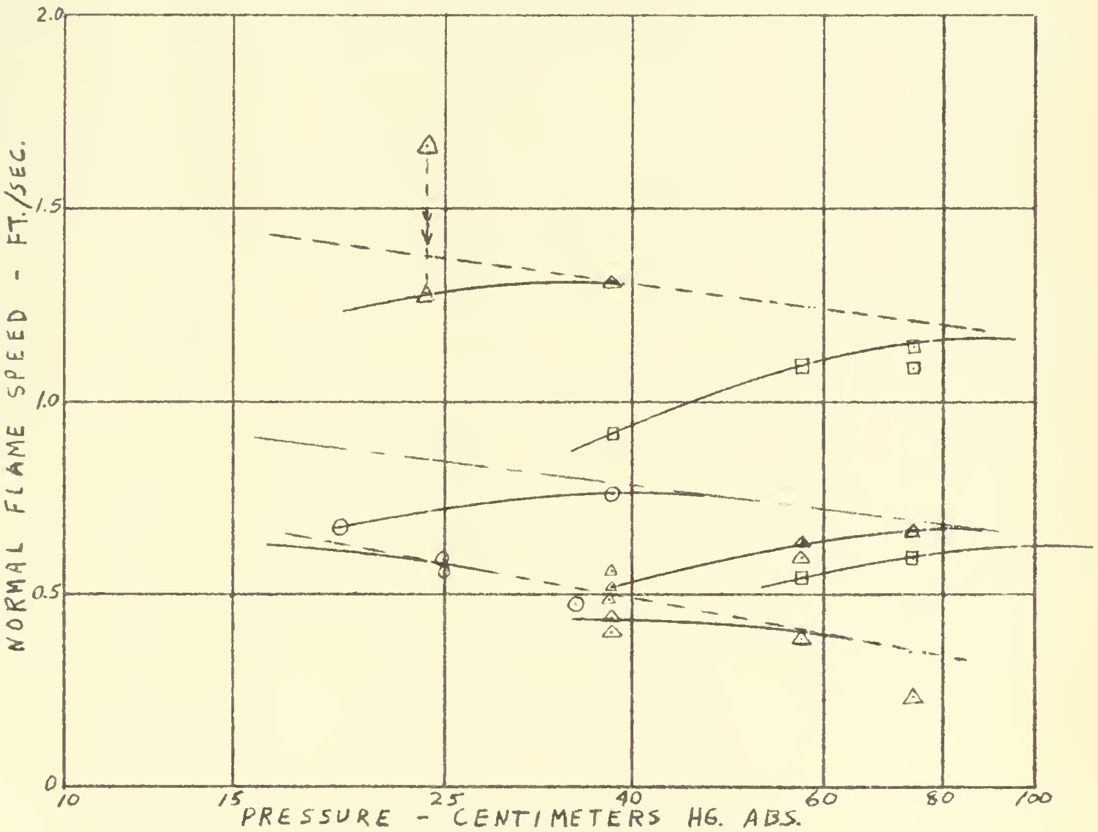

FIG. 17. GRAPH OF FLAME SPEED WITH PRESSURE FOR PROPANE - NITROGEN - OXYGEN BUNSEN FLAMES. N_2/O_2 3.76/1, 4.74/1, 5.75/1

BURNER SIZE SAME AS ETHYLENE

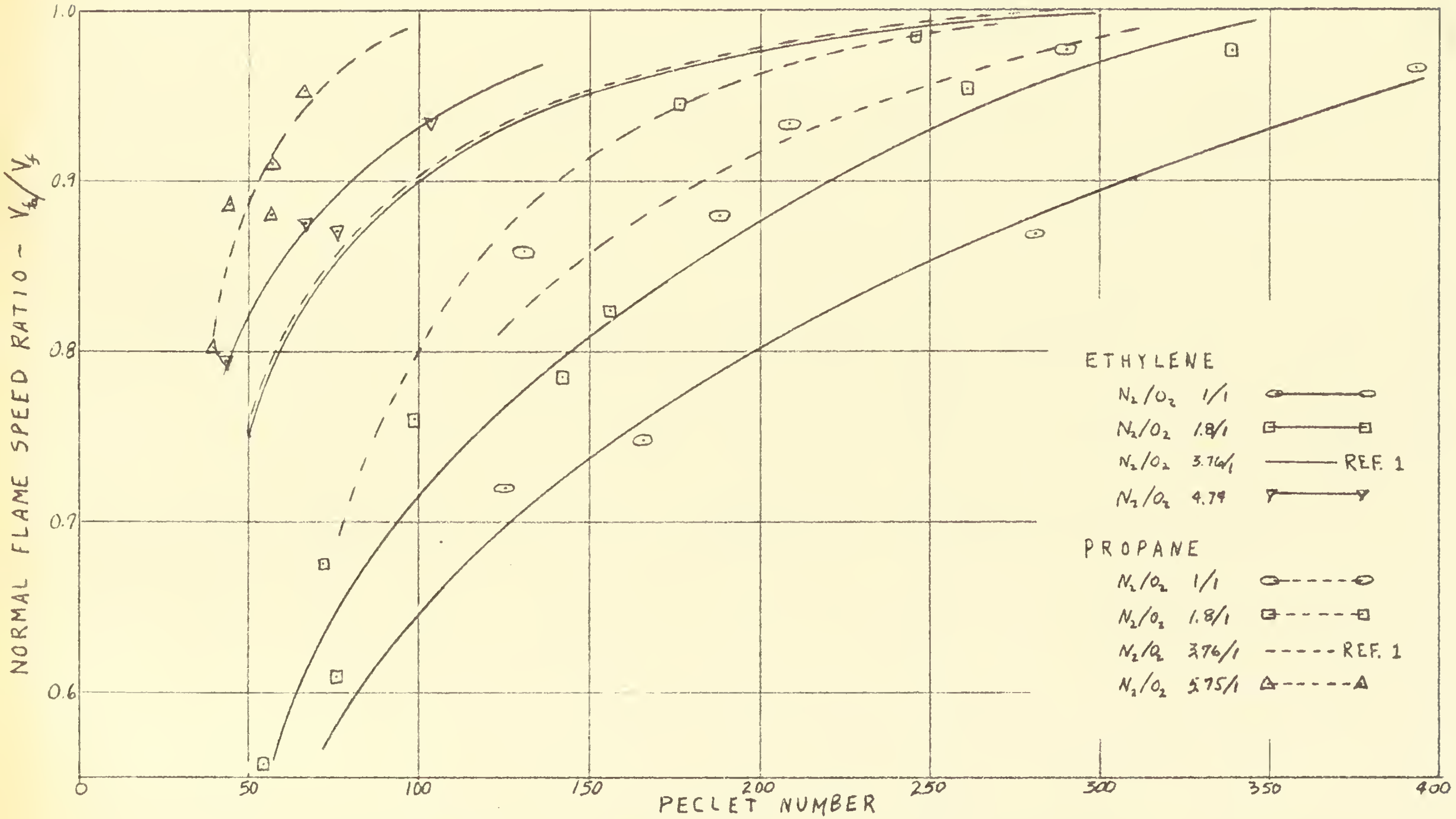

FIG. 18. GRAPH OF NORMAL FLAME SPEED RATIO (V_{f_a}/V_f) WITH PECLET NUMBER FOR CERTAIN ETHYLENE AND PROPANE NITROGEN-OXYGEN COMBINATIONS.

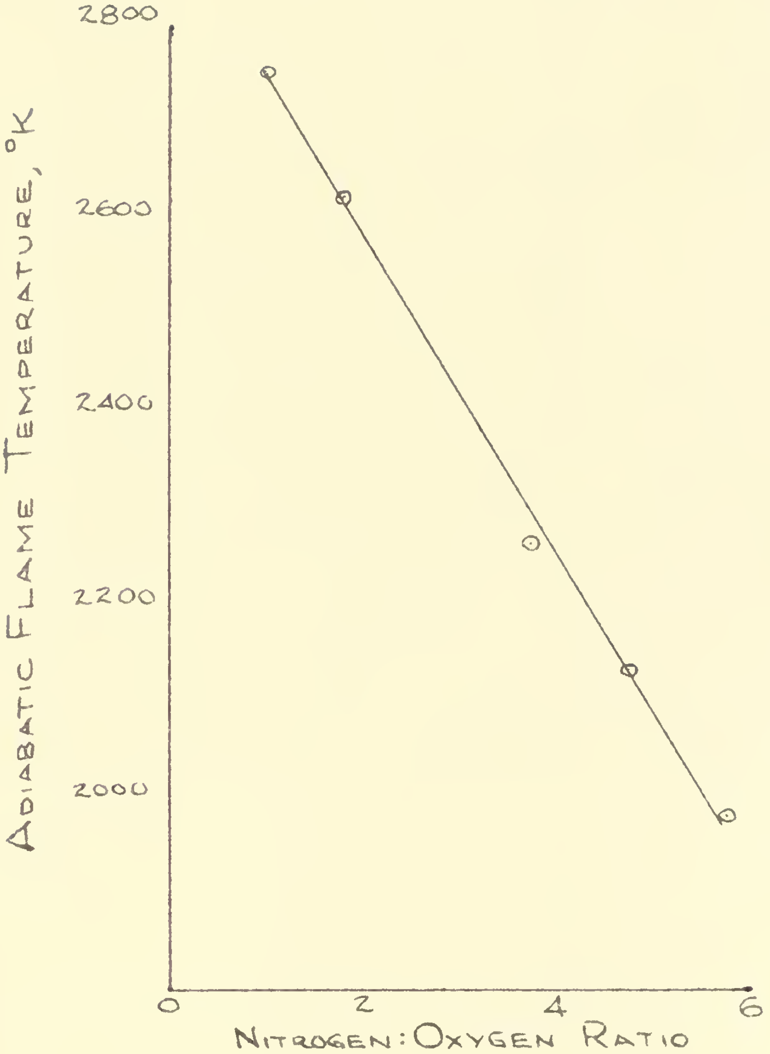

Fig. 19. Variation of Flame Temperature with Nitrogen Concentration

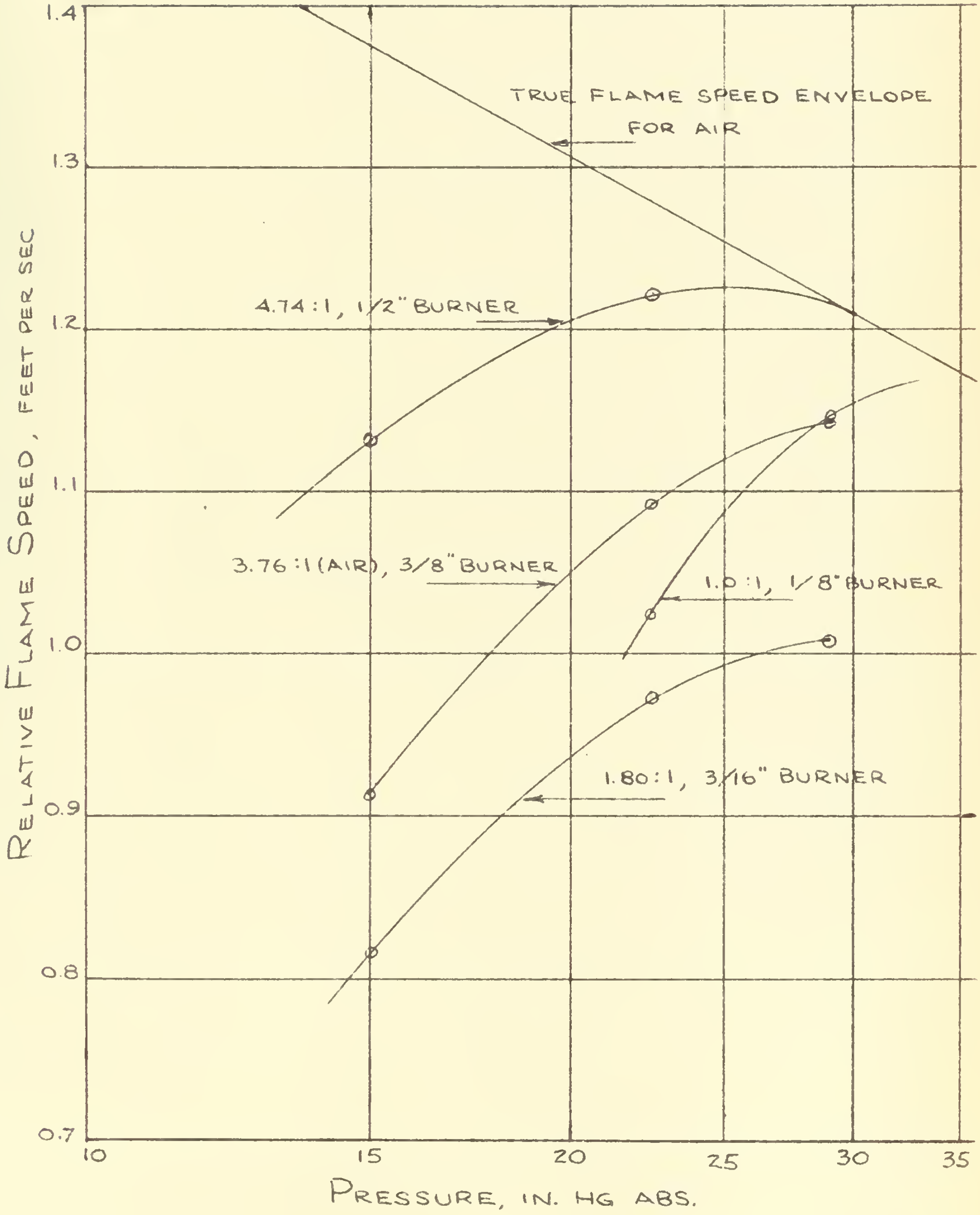

FIG. 20. VARIATION OF RELATIVE PROPANE FLAME SPEEDS WITH PRESSURE

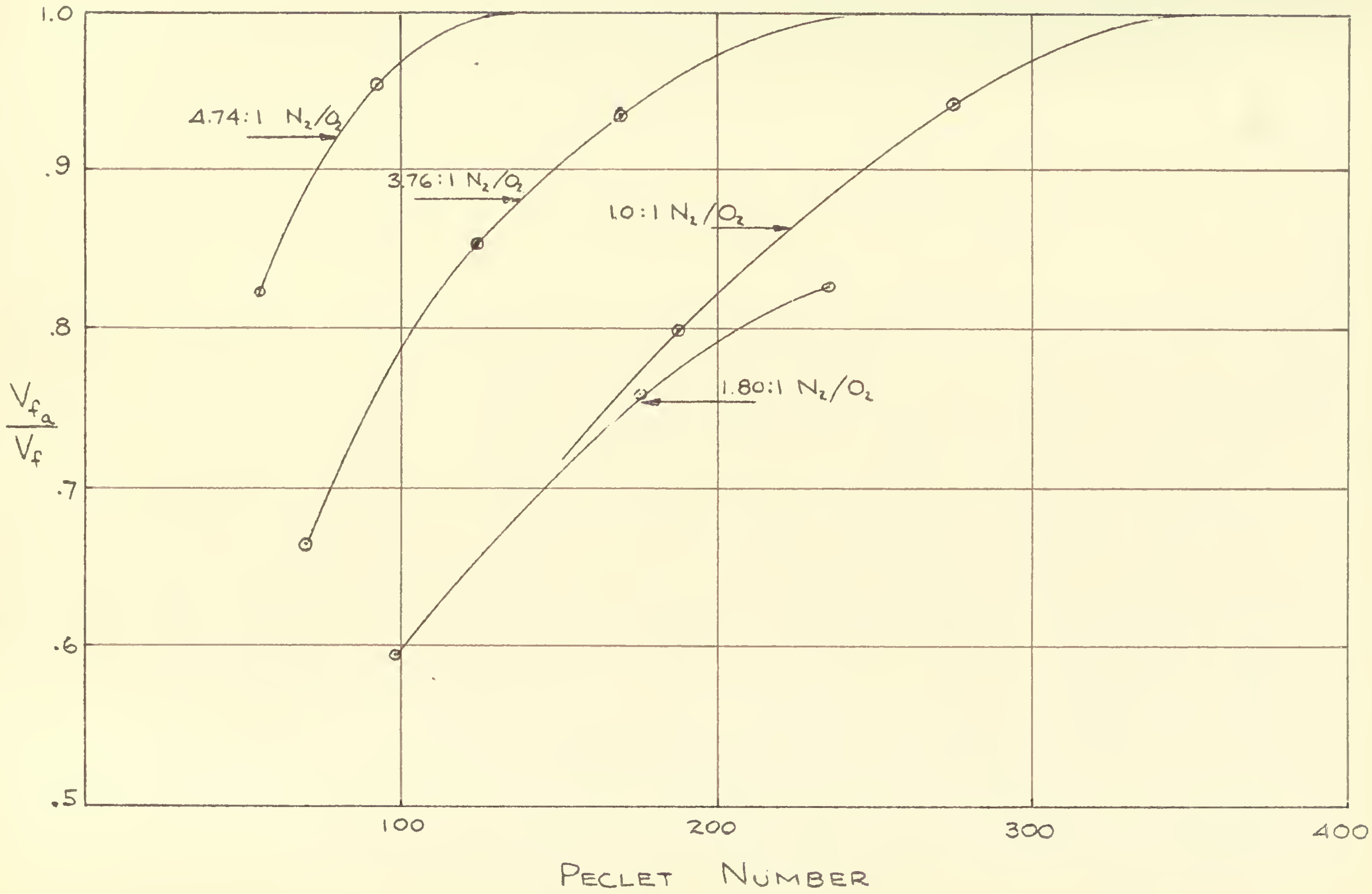

Fig. 21. Variation of Flame Speed Ratio with Peclet Number for Propane Flames and Certain Nitrogen Concentrations

APPENDIX I

SUMMARY OF RUNS

#	Fuel	N_2/O_2	Burner in.	Press. cm. hg.	A/F	O_2/F	Q_B cfm.	U_B fps.	V_f fps.	A_f in.^{2}	P_e	V'_{fa} fps.
5	C_3H_8	3.76	3/8	74.25	21.8	4.58	.160	3.23	1.14	.336	169	1.14
6	"	"	"	"	22.6	4.74	.110	2.23	1.08	.245	160	1.08
8	"	"	"	56.9	21.8	4.58	.159	3.21	1.09	.348	124	1.09
10	"	"	"	38.1	21.4	4.49	.091	1.84	.91	.239	69	.91
13	"	"	1/2	37.9	21.8	4.58	.267	3.23	1.31	.491	128	1.31
14	"	"	"	23.9	"	"	.168	2.04	1.66	.243	103	1.66
17	"	5.75	"	73.9	23.9	3.54	.054	.66	.24	.545	46	1.11
19	"	"	"	56.9	24.1	3.57	.046	.56	.39	.286	57	1.79
21	"	"	"	38.1	22.4	3.32	.044	.53	.44	.235	44	2.05
22	"	"	"	"	"	"	"	"	.40	.260	40	1.86
23	"	"	3/4	25.1	24.6	3.64	.124	.67	.56	.534	54	2.59
24	"	"	"	"	"	"	"	"	.60	.500	58	2.76
25	"	4.74	3/8	73.5	28.3	4.93	.043	.87	.59	.174	89	1.21
26	"	"	"	56.9	24.0	4.18	.056	1.14	.55	.247	64	1.12
28	"	"	1/2	73.5	29.7	5.17	.068	.83	.66	.248	128	1.35
30	"	"	"	57.0	29.4	5.12	.085	1.03	.64	.323	63	1.30
31	"	"	"	38.0	25.5	4.44	.070	.85	.49	.347	49	.99
33	"	"	"	73.55	23.2	4.06	.087	1.05	.35	.603	67	.71
35	"	"	"	57.0	25.5	4.45	"	"	.60	.348	93	1.22
37	"	"	"	38.45	23.5	4.10	.083	1.01	.55	.361	56	1.13
38	"	"	"	"	"	"	"	"	.52	.384	53	1.07
39	"	"	3/4	38.16	23.4	4.09	.186	"	.76	.590	113	1.55
40	"	"	"	19.5	23.5	4.10	.187	"	.69	.653	53	1.40
41	"	"	"	"	"	"	"	"	.66	.675	51	1.36
42	"	5.75	"	34.4	"	3.48	.127	.69	.48	.642	64	2.21
43	"	"	"	37.26	24.4	3.61	.133	.72	"	.670	69	"
45	"	3.76	"	18.96	21.8	4.58	.625	3.37	1.34	1.12	101	1.34
46	C_2H_4	"	1/4	74.48	11.7	2.45	.091	4.48	1.87	.117	172	
47	"	"	"	56.93	"	"	"	4.49	1.63	.135	114	
48	"	"	"	"	"	"	"	"	"	.134	115	
49	"	"	3/8	37.98	11.6	2.44	.223	4.48	1.88	.284	138	
50	"	"	"	"	"	"	"	"	1.89	.282	"	
52	"	"	"	18.98	"	"	.221	4.47	1.62	.328	59	
53	"	4.74	1/4	74.48	14.0	"	.041	2.00	.84	.117	76	
54	"	"	3/8	57.0	14.1	2.47	.100	2.02	.96	.251	104	
56	"	"	"	37.98	14.0	2.44	"	"	.94	.255	68	
57	"	"	"	"	"	"	"	"	.92	.260	67	
58	"	"	1/2	18.98	12.0	2.09	.146	1.76	1.05	.333	49	

#	Fuel	N_2/O_2	Burner in.	Press. cm. hg.	A/F	O_2/F	Q_B cfm.	U_B fps.	V_f fps.	A_f in.^{2}	P_e	V'_{fa} fps.
59	C_2H_4	4.74	1/2	18.98	12.0	2.09	.146	1.76	1.03	.333	48	
60	"	"	"	19.08	12.8	2.23	.153	1.85	.91	.403	43	
61	"	5.75	"	38.06	15.2	2.25	.092	1.11	.65	.341	61	
62	"	"	"	"	15.2	2.25	.092	1.11	.74	.298	69	
64	"	"	3/8	57.0	15.3	2.27	.055	1.12	.60	.220	65	
65	"	"	"	74.26	15.5	2.29	.056	1.13	.75	.179	106	
66	"	"	3/4	18.96	"	"	.279	1.51	1.12	.599	78	
67	"	"	"	"	"	"	"	"	1.09	.615	76	
68	C_3H_8	1.00	1/4	18.8	10.0	5.0	.323	15.87	4.76	.162	131	1.06
69	"	"	"	37.92	"	"	"	15.90	5.25	.148	290	1.17
71	"	"	1/8	73.8	"	"	.075	15.38	5.16	.035	275	1.15
72	"	"	"	56.95	"	"	.076	15.55	4.60	.040	188	1.02
73	"	"	3/16	38.00	"	"	.175	15.40	5.01	.084	209	1.11
74	C_2H_4	"	"	19.03	5.1	2.55	.260	22.87	6.86	.091	125	
75	"	"	1/8	74.13	"	"	.118	24.00	8.43	.034	393	
76	"	"	"	57.03	"	"	.113	23.00	7.83	.035	281	
78	"	"	"	37.93	"	"	"	23.05	6.94	.039	166	
79	"	"	"	19.2	"	"	.110	22.58	4.73	.056	57	
80	C_3H_8	1.80	3/16	73.69	14.2	5.07	.104	9.17	3.10	.081	237	1.01
81	"	"	"	57.09	"	"	"	9.15	2.98	.084	176	.97
82	"	"	"	38.04	"	"	"	9.11	2.50	.100	99	.82
84	"	"	1/4	22.39	14.3	5.11	.184	9.05	2.31	.191	72	.75
85	"	"	"	57.14	14.2	5.07	.182	8.95	3.11	.140	246	1.01
87	C_2H_4	"	3/16	57.0	6.9	2.47	.150	13.15	4.89	.073	261	
88	"	"	"	38.0	7.3	2.61	.149	13.10	4.36	.082	156	
89	"	"	"	19.0	"	"	"	13.14	3.07	.117	54	
90	"	"	"	74.7	"	"	.140	12.25	4.84	.069	339	
91	"	"	1/8	74.7	"	"	.064	13.10	4.65	.033	213	
92	"	"	"	57.0	"	"	.063	12.93	4.04	.038	142	
93	"	"	"	38.0	"	"	.065	13.22	3.23	.048	76	

APPENDIX II

SAMPLE CALCULATIONS:

The data in Table I were obtained in the following manner. Run #5 is used for the example.

	rotameter rdg.	gage pressure	Temp.
N_2/O_2	20.90	9.6 psi	74°F.
Propane	8.85	9.6	74

Flow at standard conditions was obtained from rotameter calibration curves.

N_2/O_2	0.1123 ft^3/min.
Propane	0.00515 ft^3/min.

These flows were converted to the actual flow under standard conditions by a factor converting the pressure and temperature to standard, said factor from a graph in the rotameter handbook.

Std. N_2/O_2 flow   0.1123 x 1.26 = 0.1418 ft^3/min.

Std. Propane flow   0.00515 x 1.26 = 0.0065 ft^3/min.

0.1483 ft^3/min. = $Q_{std.}$

"Air"-fuel ratio: .1418/.0065 = 21.8/1

Oxygen - fuel ratio: Air 21% O_2 by Volume

$$O_2/F = \frac{21.8 \times 0.21}{1} = 4.58/1$$

Stoichiometric equation: $C_3H_8 + 5O_2 \longrightarrow 3CO_2 + 4H_2O$

$$(O_2/F)\ \text{Stoich.} = 5/1$$

The O_2/F ratio of 4.58/1 used in run #5, the mixture which produced the best flame speed, was slightly richer than stoichiometric.

From the A/F ratio the standard density of the mixture is obtained:

Propane std. density $0.11616 \ \mathrm{lb/ft^3}$

Air std. density $0.0766 \ \mathrm{lb/ft^3}$

Mixture std. density: $$\frac{(0.11616 \times 1)+(.0766 \times 21.8)}{22.8} = .0783 \ \mathrm{lb/ft^3}$$

From gas law: $$P = \rho RT$$

$$R = P/\rho T = \frac{14.7 \times 144}{.0783 \times 520} = 52.0$$

Assuming an average burner temperature of 545°R., the density of the mixture at the burner before combustion may be calculated; $P_B = 14.38$ psi.

$$\rho_B = P_B/RT_B = \frac{14.38 \times 144}{52 \times 545} = .0732 \ \mathrm{lb/ft^3}$$

To get the actual flow at the burner, Q_B

$$\frac{\rho_{std}}{\rho_B} = \frac{Q_B}{Q_{std}} : \quad Q_B = \frac{.1483 \times .0783}{.0732} = .1585 \ \mathrm{ft^3/min.}$$

Velocity of gas at the burner, U_B:

Area of burner $= 0.1188 \ \mathrm{in}^2$

$$U_B = \frac{Q_B}{A_B} = \frac{.1585 \times 144}{.1188 \times 60} = 3.2 \ \mathrm{ft/sec.}$$

Apparent flame speed, V_{fa}:

Area of flame from photograph $= 0.336 \ \mathrm{in}^2$

$$V_{fa} = \frac{Q_B}{A_f} = \frac{.1585 \times 144}{.336 \times 60} = 1.13 \ \mathrm{ft/sec.}$$

Peclet number:

$$P_e = \frac{\rho_B \ V_{fa} \ D_B \ C_p}{K}$$

Specific heat:

$$C_{p\ air} = .25 \text{ BTU/lb}^{o}\text{F}$$

$$C_{p\ propane} = .576 \text{ BTU/lb}^{o}\text{F}$$

$$(A/F) \text{ by vol} = 21.8/1$$

$$(A/F) \text{ by wt.} = \frac{21.8 \times 28.9}{1 \times 44} = 14.45/1$$

$$C_{p\ mix} = \frac{(14.45 \times .25) + (1 \times .576)}{15.45} = 0.262 \text{ BTU/lb}^{o}\text{F}$$

Thermal Conductivity, K:

$$K \text{ air} = 424.5 \times 10^{-8} \text{ BTU/sec ft}^{o}\text{F}$$

$$K \text{ propane} = 294 \times 10^{-8} \text{ BTU/sec ft}^{o}\text{F}$$

$$K \text{ mix} = \frac{(14.45 \times 424.5) + (1 \times 294)}{15.45} 10^{-8} = 416 \times 10^{-8} \text{ BTU/sec ft}^{o}\text{F}$$

$$P_e = \frac{.0732 \times 1.13 \times .0324 \times .262}{416 \times 10^{-8}} = 169$$

Thesis
E589
33156
Erk
Effects of a diluent inert gas on ethylene and propane Bunsen flames.